nature nanotechnology

LETTERS

PUBLISHED ONLINE: 23 JUNE 2013 | DOI: 10.1038/NNANO.2013.117

Atomic clock transitions in silicon-based spin qubits

Gary Wolfowicz[1,2]*, Alexei M. Tyryshkin[3], Richard E. George[1], Helge Riemann[4], Nikolai V. Abrosimov[4], Peter Becker[5], Hans-Joachim Pohl[6], Mike L. W. Thewalt[7], Stephen A. Lyon[3] and John J. L. Morton[1,8]*

A major challenge in using spins in the solid state for quantum technologies is protecting them from sources of decoherence. This is particularly important in nanodevices where the proximity of material interfaces, and their associated defects, can play a limiting role. Spin decoherence can be addressed to varying degrees by improving material purity or isotopic composition[1,2], for example, or active error correction methods such as dynamic decoupling[3,4] (or even combinations of the two[5,6]). However, a powerful method applied to trapped ions in the context of atomic clocks[7,8] is the use of particular spin transitions that are inherently robust to external perturbations. Here, we show that such 'clock transitions' can be observed for electron spins in the solid state, in particular using bismuth donors in silicon[9,10]. This leads to dramatic enhancements in the electron spin coherence time, exceeding seconds. We find that electron spin qubits based on clock transitions become less sensitive to the local magnetic environment, including the presence of ^{29}Si nuclear spins as found in natural silicon. We expect the use of such clock transitions will be of additional significance for donor spins in nanodevices[11], mitigating the effects of magnetic or electric field noise arising from nearby interfaces and gates.

Of the various candidates for solid-state qubits, spins have been of particular interest due to their relative robustness to decoherence compared with other degrees of freedom, such as charge. The most coherent solid-state systems investigated so far are the spins of well-isolated donors in bulk ^{28}Si, which produce coherence times (T_2) of up to seconds (extrapolated) for the electron spin[1] and minutes for the nuclear spin[5], which are comparable to those of ion trap qubits[12,13]. However, in practical devices, spin coherence times are likely to be limited by factors such as coupling to nearby qubits and magnetic or electric field noise from the environment. For example, cross-talk with other donors 100 nm away limits the electron spin T_{2e} to a few milliseconds[1], while a nearby interface can limit the donor electron spin T_{2e} to 0.3 ms at 5.2 K (ref. 14). Furthermore, without isotopic enrichment, the 5% natural abundance of ^{29}Si limits the electron spin T_{2e} to less than 1 ms (refs 9,10).

One approach to creating more robust qubits is to tune the free parameters of the system Hamiltonian to produce insensitivity to specific sources of decoherence. This has been used extensively in ion trap qubits to protect against magnetic field fluctuations[12,13], building on work on atomic clocks where hyperfine transitions, used as frequency standards, must remain stable against such variations. These so-called clock transitions have a transition frequency f that is insensitive to variations in the magnetic field B, at least to first order (in other words, $\mathrm{d}f/\mathrm{d}B = 0$). More recently, superconducting circuit qubits have also taken advantage of a tuned Hamiltonian to remain immune to charge, flux or current noise[15,16].

Nuclear spin clock transitions in rare-earth dopants (nuclear spins $I > 5/2$) have been studied in the context of optical quantum memories[17,18], leading to a 600-fold improvement of the coherence times to 150 ms, limited by second-order effects. Recent experiments on phosphorus donor nuclear spins have also exploited a clock transition[5]. For electron spins in the solid state, clock transitions remain relatively unused due in part to the requirement for a spin Hamiltonian of sufficient complexity. One of the richest single-defect spin systems is the Bi donor in Si (Si:Bi), which has an electron spin $S = 1/2$ coupled to a nuclear spin $I = 9/2$. The electron spin decoherence rates for Si:Bi have been found to follow $\mathrm{d}f/\mathrm{d}B$ both in natural silicon[9] and in isotopically enriched ^{28}Si (ref. 19). These results, combined with the identification of a number of clock transitions in the spin Hamiltonian of Si:Bi (ref. 20), motivate the study of spin coherence times around clock transitions in Si:Bi, where $\mathrm{d}f/\mathrm{d}B \to 0$. In this Letter, we investigate one such clock transition in Si:Bi, at 7.0317 GHz, using both natural Si and ^{28}Si.

When describing the states of coupled electron and nuclear spins, two basis conventions are typically used. In the high-magnetic-field limit, the electron and nuclear spin projections m_S and m_I are good quantum numbers, whereas in the zero-field limit, the total spin F ($= I \pm S$) and its projection m_F ($= m_S + m_I$) are used. Clock transitions are often found in an intermediate regime; nevertheless, it is possible to categorize them as NMR-type or electron spin resonance (ESR)-type, on the basis of whether the transition couples primarily to S_x or I_x, where these are the electron and nuclear spin operators perpendicular to the applied magnetic field. The ESR-type clock transitions investigated in this Letter involve states that are close to pure in the $|F,m_F\rangle$ basis, so for convenience we label them according to the dominant $|F,m_F\rangle$ component (full details are given in Supplementary Section S1 and in ref. 20). It is important to note that the extended coherence time expected at a clock transition is not a feature of electron–nuclear spin hybridization alone: for example, ESR measurements of Si:Bi at 4 GHz, where the electron and nuclear spin are strongly mixed[21], showed no enhancement in coherence time compared with those measured at 10 GHz, where the spin states were close to pure[9].

For Bi donors in Si, NMR-type clock transitions can be found at high fields (>350 mT) with frequencies around 1 GHz, as shown in red in Fig. 1a. At low fields (<200 mT), four ESR-type clock

[1]London Centre for Nanotechnology, University College London, London WC1H 0AH, UK, [2]Department of Materials, Oxford University, Oxford OX1 3PH, UK, [3]Department of Electrical Engineering, Princeton University, Princeton, New Jersey 08544, USA, [4]Institute for Crystal Growth, Max-Born Strasse 2, D-12489 Berlin, Germany, [5]Physikalisch-Technische Bundesanstalt, D-38116 Braunschweig, Germany, [6]Vitcon Projectconsult GmbH, 07745 Jena, Germany, [7]Department of Physics, Simon Fraser University, Burnaby, British Columbia V5A 1S6, Canada, [8]Department of Electronic & Electrical Engineering, University College London, London WC1E 7JE, UK. *e-mail: gary.wolfowicz@materials.ox.ac.uk; jjl.morton@ucl.ac.uk

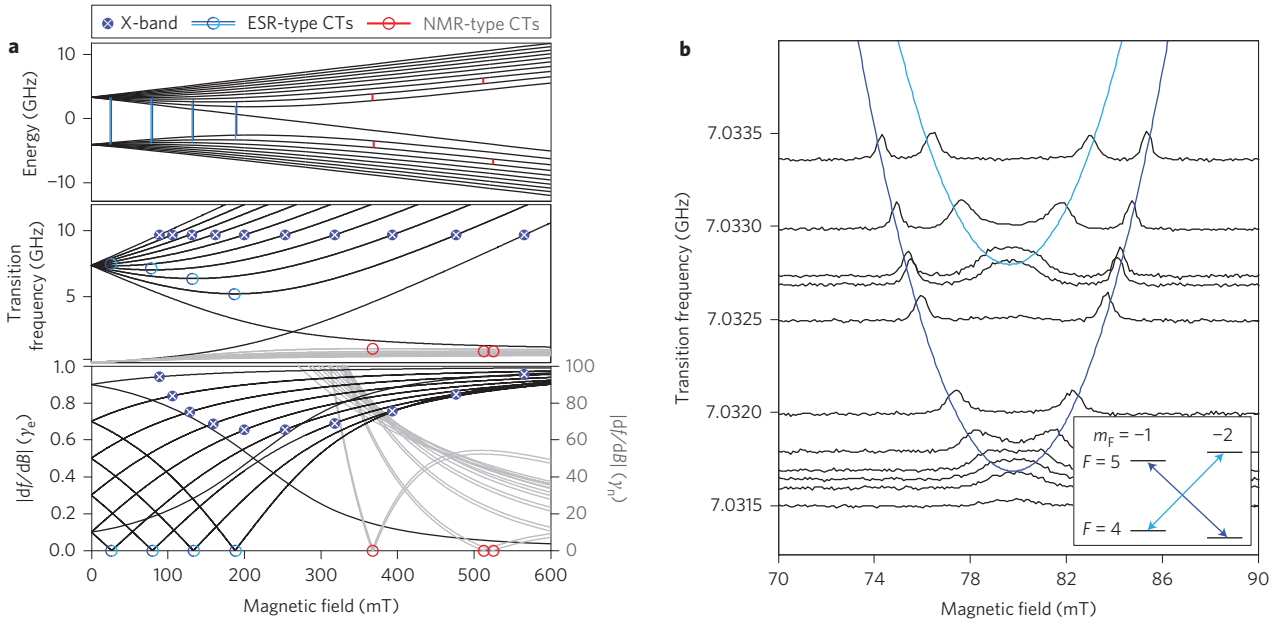

Figure 1 | ESR-type clock transitions (CTs) of Si:Bi. a, Top: eigenstate energies of Si:Bi as a function of magnetic field. Middle: ESR- (black) and NMR-type (grey) transition frequencies between these states. Bottom: first-order magnetic field dependence (df/dB) of these transition frequencies. ESR-type clock transitions (blue lines and open circles) are found at 27, 80, 133 and 188 mT, and appear in the spectrum as doublets $\Delta F\Delta m_F = \pm 1$ separated by up to 3 MHz. NMR-type clock tranistions are found above 300 mT (red lines and open circles). **b**, The electron spin echo-detected magnetic field sweeps around the 80 mT clock transition measured at microwave frequencies $\geq$7.0315 GHz. The transition probablities for $\Delta F\Delta m_F = +1$ (dark blue) and -1 (light blue) transitions are equal near the clock transition.

transitions are present with frequencies in the range 5.2–7.3 GHz, as shown in blue in Fig. 1a. We will focus here on the ESR-type clock transitions, which have only a slightly reduced spin manipulation time compared with free electron spins, as well as large energy splitting even at low magnetic field (which has interesting applications in hybrid superconducting circuits[9,22,23]).

In the Si samples we study here, Bi donors were introduced during crystal growth using the method developed in ref. 24, with concentrations ranging from 3.6×10^{14} cm^{-3} to 4.4×10^{15} cm^{-3}. Pulsed-ESR experiments were performed using a spectrometer based around a modified Bruker Elexsys E580 system with an ~7 GHz loop-gap cavity (for the clock transition) and 9.75 GHz dielectric resonator.

Figure 1b presents ESR spectra measured using microwave frequencies between 7.031 and 7.034 GHz, by plotting electron spin echo intensity as a function of magnetic field. The spectra show two transitions corresponding to $[\{\Delta F, \Delta m_F\} = \{\pm 1, \pm 1\}]$ and $[\{\Delta F, \Delta m_F\} = \{\pm 1, \mp 1\}]$; for brevity, these transitions can be distinguished by the value of the product $\Delta F\Delta m_F = \pm 1$. Together, they offer a controllable two-qubit subsystem with low sensitivity to magnetic field fluctuations (Fig. 1b, inset).

We model the ESR spectra using an isotropic spin Hamiltonian common for group V donors in silicon:

$$H_0 = B_0(\gamma_e S_z - \gamma_n I_z) + A\mathbf{S}.\mathbf{I}$$

where the two first terms correspond to the electronic (S) and nuclear (I) spin Zeeman interactions with an external field B_0 and the last term corresponds to the hyperfine coupling A. A common way to estimate Hamiltonian parameters such as the electron and nuclear gyromagnetic ratios (γ_e and γ_n) and the hyperfine constant is to measure the magnetic field dependencies of the spin transition frequencies. We use the opportunity provided by the clock transition (with $df/dB \to 0$) to extract a measure of the mean hyperfine constant $A = 1.475169(7)$ GHz with high precision, because uncertainties in the magnetic field become irrelevant. In our simulations, we also use the previously reported value of $\gamma_e = 27.997(1)$ GHz T^{-1} (ref. 25), and γ_n for ^{209}Bi is a fitting parameter with a value of 6.9(2) MHz T^{-1} (Supplementary Section S4).

Figure 1b shows that the ESR linewidth in the magnetic field domain increases around the clock transition: the derivative df/dB tends to zero, so its inverse, dB/df, diverges until it becomes limited by the nonlinear terms in $f(B_0)$. These spectra are all well fit assuming a constant linewidth in the frequency domain of 270 kHz. This linewidth can be attributed to a distribution in the hyperfine constant of ~60 kHz, using $\Delta f = (df/dA)\Delta A$ at the clock transition, due to strains in the lattice. Fourier-transform ESR performed at a range of magnetic fields confirmed that the ESR linewidth in the frequency domain is indeed magnetic field-independent (Supplementary Section S3).

We now examine the decoherence mechanisms that affect the electron spin of donors in Si. At a sufficiently low temperature (<5 K), spin-lattice relaxation T_{1e} can be mostly neglected, and dipolar interactions ($\sim 2S_zS_z - (S_xS_x + S_yS_y)$) with neighbouring spins are the primary source of decoherence. In a central spin representation, as shown in Fig. 2a, the surrounding spins can be divided into three categories: (i) resonant spins affected by microwave excitation; (ii) off-resonant spins of the same species, that is, Bi spins in m_F levels not addressed by the microwaves; and (iii) other spin species such as ^{29}Si. Away from clock transitions, the limiting factor for electron spin coherence times is spectral diffusion from the S_zS_z term of the dipolar interaction. This term can be assimilated into effective fluctuations in the magnetic field environment of the central spin. Spectral diffusion is independent of any frequency detuning between spins and is therefore valid between the central spin and any others.

In the static case, dipolar couplings to (ii) and (iii) can be refocused with a microwave π-pulse such as in the Hahn echo sequence. However, this does not correct for dipolar coupling between resonant spins (i), as both spins are simultaneously flipped by the π-pulse. This is called 'instantaneous diffusion' and limits T_{2e} to ~10–100 ms for typical donor concentrations ($>1 \times 10^{14}$ cm^{-3})

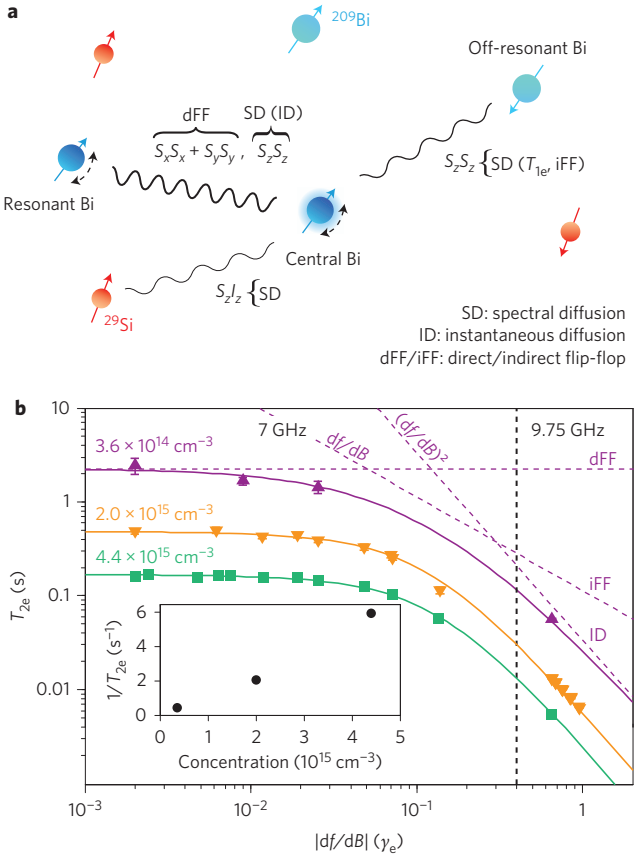

Figure 2 | Decoherence mechanisms of Bi donors in Si and their dependence on df/dB. a, In the central spin representation, a Bi donor is coupled to neighbouring Bi donors as well as ^{29}Si spins. At the ESR clock transition, all SD contributions to decoherence are essentially eliminated, leaving only the dFF between the central spin and a neighbouring, resonant Bi spin. **b**, T_{2e} measurements at 4.8 K show a strong dependence on df/dB, as shown for three different donor concentrations in ^{28}Si :Bi. Measurements close to df/d$B = \gamma_e$ were taken using the ten X-band ESR transitions, while the remaining points were taken close to the clock transition. For each concentration, the dependence on df/dB is modelled using contributions from ID, iFF and dFF, as shown separately as dashed lines for the lowest concentration. Inset: the limit of $1/T_{2e}$ when approaching the exact clock transition as a function of donor concentration, showing a nearly linear dependence, as expected for dFF.

(refs 1,19). (By reducing the microwave power and effectively flipping only a small part of the resonant spins it is possible to obtain an extrapolation of coherence times in the limit of no instantaneous diffusion[26]; however, this is not a solution to overcoming the effect of instantaneous diffusion in practice.) Furthermore, dynamic changes from spin flips in the environment cannot be refocused. At high temperatures, such flips arise from phonon scattering, but at low temperatures, this is due to flip-flops from the $S_xS_x + S_yS_y$ term of the dipolar interaction. Flip-flops are energy conserving and, as such, are only relevant between spins that have similar transition frequencies. In natural silicon, the dominant decoherence mechanism is spectral diffusion from ^{29}Si flip-flops, whereas in isotopically enriched ^{28}Si, it arises from flip-flops between resonant Bi spin pairs. In the latter case, we distinguish between flip-flops that involve the central spin (direct flip-flops, dFFs) and those that do not (indirect flip-flops, iFFs).

We begin by discussing results on samples of isotopically enriched ^{28}Si (100 ppm ^{29}Si). At the clock transition, the transition frequency is insensitive to magnetic field fluctuations in first order,

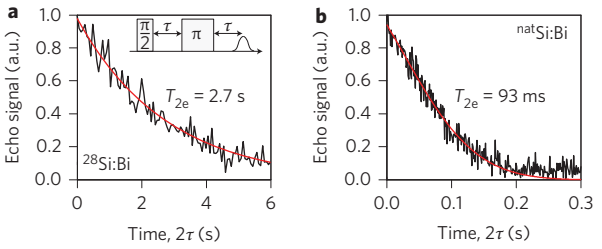

Figure 3 | Hahn echo decay at the clock transition. a, ^{28}Si:Bi at 4.3 K with a Bi concentration of 3.6×10^{14} cm^{-3}. The decay in ^{28}Si is exponential (fit in red). **b**, ^{nat}Si:Bi at 4.8 K with a Bi concentration of 1×10^{15} cm^{-3}. The decay in natural Si is a stretched exponential (fit in red), so T_{2e} is defined as the time when the amplitude reaches 1/e. Magnitude detection was used to eliminate instrumental noise that was probably due to phase noise in the microwave source.

so we expect spectral diffusion to have little effect, leaving only the dipolar coupling between resonant spin pairs. With reference to Fig. 2a, this then implies that all terms apart from dFFs vanish. In Fig. 2b, measurements of electron spin coherence times (T_{2e}) are shown for three different concentrations over a wide range of df/dB. The data include values measured at the X-band as well as those near the clock transition ($\Delta F \Delta m_F = +1$) at 79.8 mT, 7.0317 GHz. Measurements at the clock transition shown here were taken at 4.8 K where $T_{1e} = 9$ s; however, no increase in T_{2e} was seen at lower temperatures.

For each sample, enhancements of about two orders of magnitude are seen at the clock transition compared to the case for a free electron g-factor, such as that of P donors. As shown in Fig. 2b, the dependence of the measured T_{2e} on df/dB arises from two factors: the effects on instantaneous diffusion and on iFF. Instantaneous diffusion has a known quadratic dependence on the gyromagnetic ratio of the central spin[19,27], and becomes a negligible effect for df/d$B < 0.1\gamma_e$. iFFs dephase the central spin through the S_zS_z term, giving a linear dependence of T_{2e} on df/dB. dFFs, on the other hand, are not eliminated at the clock transition and provide an upper bound on T_{2e} for a given donor spin concentration, as plotted in the inset of Fig. 2b. The solid curves shown are based on a model that combines these three different decoherence processes, as described in more detail in the Supplementary Information. For the lowest-concentration sample, electron spin coherence times of up to 2.7 s were measured from simple two-pulse Hahn echo decays, as shown in Fig. 3a.

We now turn to measurements on Bi-doped natural Si (^{nat}Si:Bi), which has 5% ^{29}Si. Away from the clock transition the effect of the ^{29}Si ($I = 1/2$) is to broaden the ESR linewidth to ~0.4 mT (equivalent to 12 MHz in the frequency domain for a free electron) due to unresolved ^{29}Si hyperfine coupling, as well as to limit the T_{2e} to ~0.8 ms due to spectral diffusion[9]. At the clock transition we find that the ESR linewidth reduces to 500 kHz (Supplementary Section S2), within a factor of two of the value for enriched ^{28}Si material, while T_{2e} increases by over two orders of magnitude to ~90 ms (Fig. 3b). The effect of the suppression of spectral diffusion around the clock transition has been simulated for ^{nat}Si:Bi using cluster expansion methods[28], although further refinements are required in the simulation before a quantitative comparison can be made. The stretched-exponential decay implies that T_{2e} is still limited at 93 ms by spectral diffusion from ^{29}Si due to the second-order term ($d^2f/dB^2 \neq 0$). For modest ^{28}Si enrichment (for example, [^{29}Si] ≈ 1,000 ppm), T_{2e} should already exceed seconds, and indeed there may be an optimal ^{28}Si purity above which T_{2e} at the clock transition drops, due to the role of ^{29}Si or ^{30}Si in detuning otherwise identical spins[29]. Alternatively, it is possible to combine the use of a clock transition with dynamical decoupling methods[30], and this could be used to extend T_{2e} in ^{nat}Si:Bi.

We have shown how clock transitions in Si:Bi can be used to produce magnetic field-insensitive spin qubits with directly measured coherence times of several seconds. Such qubits would be insensitive to magnetic field noise arising, for example, from fluctuating dangling-bond spins at the Si/SiO_2 interface. Conversely, if electric field noise is dominant, this can couple to donor spins via the hyperfine interaction and cause decoherence. Again, clock transitions can be designed to be immune from electric charge noise by selecting points where $df/dA \rightarrow 0$ (see Supplementary Information). Through the use of clock transitions, it is likely that the seconds-long electron spin coherence times measured in the bulk can be harnessed for spins in practical quantum devices.

Received 4 March 2013; accepted 22 May 2013;
published online 23 June 2013

References

1. Tyryshkin, A. M. *et al.* Electron spin coherence exceeding seconds in high-purity silicon. *Nature Mater.* **11,** 143–147 (2012).
2. Balasubramanian, G. *et al.* Ultralong spin coherence time in isotopically engineered diamond. *Nature Mater.* **8,** 383–387 (2009).
3. Viola, L. & Lloyd, S. Dynamical suppression of decoherence in two-state quantum systems. *Phys. Rev. A* **58,** 2733–2744 (1998).
4. Bluhm, H. *et al.* Dephasing time of GaAs electron-spin qubits coupled to a nuclear bath exceeding 200 μs. *Nature Phys.* **7,** 109–113 (2011).
5. Steger, M. *et al.* Quantum information storage for over 180 s using donor spins in a ^{28}Si 'semiconductor vacuum'. *Science* **336,** 1280–1283 (2012).
6. Maurer, P. C. *et al.* Room-temperature quantum bit memory exceeding one second. *Science* **336,** 1283–1286 (2012).
7. Bollinger, J., Prestage, J., Itano, W. & Wineland, D. Laser-cooled-atomic frequency standard. *Phys. Rev. Lett.* **54,** 1000–1003 (1985).
8. Fisk, P. T. H. *et al.* Very high Q microwave spectroscopy on trapped $^{171}Yb^{+}$ ions: application as a frequency standard. *IEEE Trans. Instrum. Meas.* **44,** 113–116 (1995).
9. George, R. E. *et al.* Electron spin coherence and electron nuclear double resonance of Bi donors in natural Si. *Phys. Rev. Lett.* **105,** 067601 (2010).
10. Morley, G. W. *et al.* The initialization and manipulation of quantum information stored in silicon by bismuth dopants. *Nature Mater.* **9,** 725–729 (2010).
11. Pla, J. J. *et al.* A single-atom electron spin qubit in silicon. *Nature* **489,** 541–545 (2012).
12. Haljan, P. *et al.* Entanglement of trapped-ion clock states. *Phys. Rev. A* **72,** 062316 (2005).
13. Langer, C. *et al.* Long-lived qubit memory using atomic ions. *Phys. Rev. Lett.* **95,** 060502 (2005).
14. Schenkel, T. *et al.* Electrical activation and electron spin coherence of ultralow dose antimony implants in silicon. *Appl. Phys. Lett.* **88,** 112101 (2006).
15. Vion, D. *et al.* Manipulating the quantum state of an electrical circuit. *Science* **296,** 886–889 (2002).
16. Koch, J. *et al.* Charge-insensitive qubit design derived from the Cooper pair box. *Phys. Rev. A* **76,** 042319 (2007).
17. Longdell, J., Alexander, A. & Sellars, M. Characterization of the hyperfine interaction in europium-doped yttrium orthosilicate and europium chloride hexahydrate. *Phys. Rev. B* **74,** 195101 (2006).
18. McAuslan, D., Bartholomew, J., Sellars, M. & Longdell, J. Reducing decoherence in optical and spin transitions in rare-earth-metal-ion-doped materials. *Phys. Rev. A* **85,** 032339 (2012).
19. Wolfowicz, G. *et al.* Decoherence mechanisms of ^{209}Bi donor electron spins in isotopically pure ^{28}Si. *Phys. Rev. B* **86,** 245301 (2012).
20. Mohammady, M. H., Morley, G. W., Nazir, A. & Monteiro, T. S. Analysis of quantum coherence in bismuth-doped silicon: a system of strongly coupled spin qubits. *Phys. Rev. B* **85,** 094404 (2012).
21. Morley, G. W. *et al.* Quantum control of hybrid nuclear–electronic qubits. *Nature Mater.* **11,** 1–5 (2012).
22. Schuster, D. *et al.* High-cooperativity coupling of electron–spin ensembles to superconducting cavities. *Phys. Rev. Lett.* **105,** 140501 (2010).
23. Kubo, Y. *et al.* Storage and retrieval of a microwave field in a spin ensemble. *Phys. Rev. A* **85,** 012333 (2012).
24. Riemann, H., Abrosimov, N. & Noetzel, N. Doping of silicon crystals with Bi and other volatile elements by the pedestal growth technique. *ECS Trans.* **3,** 53–59 (2006).
25. Feher, G. Electron spin resonance experiments on donors in silicon. I. Electronic structure of donors by the electron nuclear double resonance technique. *Phys. Rev.* **114,** 1219–1244 (1959).
26. Salikhov, K., Dzuba, S. & Raitsimring, A. The theory of electron spin-echo signal decay resulting from dipole–dipole interactions between paramagnetic centers in solids. *J. Magn. Reson.* **42,** 255276 (1981).
27. Schweiger, A. & Jeschke, G. *Principles of Pulse Electron Paramagnetic Resonance* Ch. 8.1.5, 216 (Oxford Univ. Press, 2001).
28. Balian, S. J. *et al.* Measuring central-spin interaction with a spin-bath by pulsed ENDOR: towards suppression of spin diffusion decoherence. *Phys. Rev. B* **86,** 104428 (2012).
29. Witzel, W., Carroll, M., Morello, A., Cywinski, L. & Das Sarma, S. Electron spin decoherence in isotope-enriched silicon. *Phys. Rev. Lett.* **105,** 187602 (2010).
30. Fraval, E., Sellars, M. & Longdell, J. Dynamic decoherence control of a solid-state nuclear-quadrupole qubit. *Phys. Rev. Lett.* **95,** 030506 (2005).

Acknowledgements

The authors thank S. Simmons, T. Monteiro and S. Balian for discussions. This research is supported by the Engineering and Physical Sciences Research Council through the Materials World Network (EP/I035536/1) and a Doctoral Training Award, as well as by the European Research Council under the European Community's Seventh Framework Programme (FP7/2007–2013)/ERC (grant agreement no. 279781). Work at Princeton was supported by the National Science Foundation through Materials World Network (DMR-1107606) and through the Princeton Materials Research Science and Engineering Center (DMR-0819860) and the National Security Agency/Laboratory for Physical Sciences through Lawrence Berkley National Laboratory (6970579). J.J.L.M. is supported by the Royal Society.

Author contributions

G.W., A.M.T., R.E.G., S.A.L., M.L.W.T. and J.J.L.M. conceived and designed the experiments. G.W. and A.M.T. performed the experiments. G.W., A.M.T., S.A.L. and J.J.L.M. analysed the data. H.R., N.V.A., P.B., H-J.P. and M.L.W.T. provided materials. G.W. and J.J.L.M. wrote the paper with input from all authors.

Additional information

Supplementary information is available in the online version of the paper. Reprints and permissions information is available online at www.nature.com/reprints. Correspondence and requests for materials should be addressed to G.W. and J.J.L.M.

Competing financial interests

The authors declare no competing financial interests.